2005-01-2930

Detection of Smoke from Microgravity Fires

David Urban, DeVon Griffin, Gary Ruff
NASA Glenn Research Center

Thomas Cleary, Jiann Yang, George Mulholland
National Institute of Standards and Technology

Zeng-guang Yuan
National Center for Microgravity Research

Copyright © 2005 SAE International

ABSTRACT

The history and current status of spacecraft smoke detection is discussed including a review of the state of understanding of the effect of gravity on the resultant smoke particle size. The results from a spacecraft experiment (Comparative Soot Diagnostics (CSD)) which measured microgravity smoke particle sizes are presented. Five different materials were tested producing smokes with different properties including solid aerosol smokes and liquid droplets aerosol smokes. The particulate size distribution for the solid particulate smokes increased substantially in microgravity and the results suggested a corresponding increase for the smokes consisting of a liquid aerosol. A planned follow on experiment that will resolve the issues raised by CSD is presented. Early results from this effort have provided the first measurements of the ambient aerosol environment on the ISS (International Space Station) and suggest that the ISS has very low ambient particle levels.

INTRODUCTION

The non-buoyant microgravity environment causes substantial changes in flame structure and consequently changes the properties of the produced smoke. In particular, the increased residence time in the high temperature zone where the smoke is formed, increases the opportunity for growth in the size of the smoke particulate. This change has hampered the rational implementation of spacecraft smoke detectors because there is very little data concerning the resultant size of microgravity smoke particulate and the background dust aerosol size distribution. In the absence of any reference data, the ISS and STS (Space Transportation System or Space Shuttle) Orbiter smoke detectors each were designed using different detection technologies which have very different particle size sensitivities.

SMOKE BACKGROUND – Smoke is a general term that encompasses aerosol materials produced by a number of processes. In particular it can include unburned, recondensed, original polymer or pyrolysis products that can be either liquid or solid, hydrocarbon soot, condensed water vapor, and ash particles. Ash particles and soot particles are the dominant particulate in established fires while early ignition and fire establishment periods tend to produce higher concentrations of unburned pyrolysis products and recondensed polymer fragments. Given the constrained environment on any spacecraft the target for any detection system is necessarily the early ignition period and not after the fire has become established, consequently, the primary target for detection is the pyrolysis products and not the soot and ash.

PRIOR SPACECRAFT SYSTEMS - In the earliest missions (Mercury, Gemini and Apollo), the crew quarters were so cramped that it was considered reasonable that the astronauts would rapidly detect any fire. The Skylab module, however, included approximately 30 UV-sensing fire detectors (Friedman, 1992). These devices were limited to line-of sight and were reported to have difficulties with false alarms.

<u>Space Shuttle Detectors</u> - The Space Shuttle Orbiter was developed in a time (1970's) of rapid progress in smoke detection for terrestrial applications (Bukowski and Mulholland, 1978). At the time, ionization detectors were becoming readily available but photoelectric (scattering or obscuration detectors) were generally unavailable due to the difficulty of producing stable light sources. There was no data available concerning the smoke particle size distribution in low-gravity and the database of normal-gravity smoke characteristics was a fraction of what is available today. There was also no data on spacecraft dust particle size distributions but the absence of gravitational settling suggested that there would be more large particles than are seen on earth. Consequently it is understandable that the Orbiter

design (figure 1) employed a variant of the accepted ground based approach (ionization detectors). The Orbiter has 9 particle-ionization smoke detectors in avionics cooling air return lines in the mid-deck and flight deck and SpaceLab had six additional particle-ionization smoke detectors in the avionics lines. (Martin and DaLee 1993) While the design rationale is not completely known, Celesco™ (later Brunswick Defense™) based their design on data that suggested incipient fires could be discriminated by looking for particulate in the 0.4 to 0.7 μm range (L.G. Barr in National Research Council 1975). Use of a pump provided the opportunity to employ a particle separator allowing rejection of particulate larger than 1μm consistent with their understanding that incipient smoke particles were smaller than 1 μm. Furthermore, since the response from ionization chambers is affected by the ambient air velocity, implementing an ionization detector in a flow duct was probably facilitated by the use of an air pump to control the air flow through the smoke detector. This air pump increased the power requirements and reduced the operational life for the detectors.

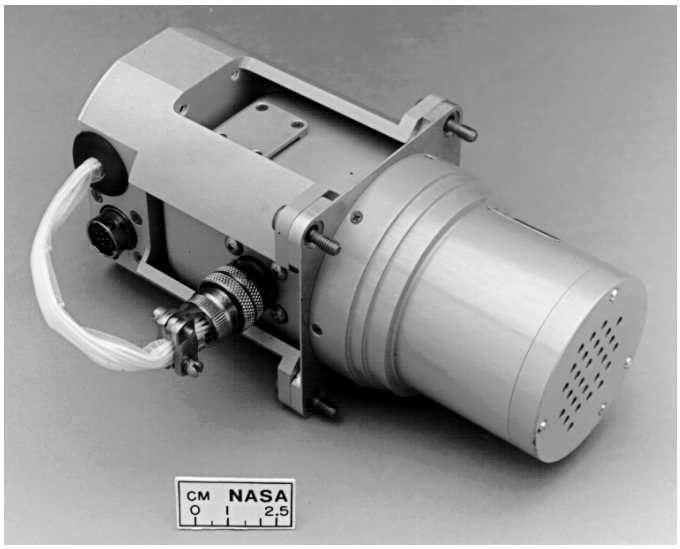

Figure 1: Brunswick Defense™ smoke detector used in the NASA orbiter fleet. The inlet is on the right and the gas is expelled out the small plate on the top.

ISS Detectors - At the time the International Space Station (ISS) was being developed, stable laser-diode light sources were readily available. Consequently, terrestrial smoke detectors using light scattering were becoming more readily available. This provided the opportunity to produce a detector that required substantially less power, (1.5 Watts versus 9 Watts for the orbiter detector) (Steisslinger et al., 1993) and, with no moving parts, was quieter with a much longer operational life. The choice was supported by data indicating that early smoldering fires produce larger particulate than established flaming fires (Bukowski and Mulholland, 1978). The designated detectors (figure 2) for the ISS are laser-diode, forward-scattering, smoke or particulate detectors. Their sensitivity is greatest for particles larger than 1 μm with sensitivity extending down to 0.6 μm. The current requirements for the ISS call for two detectors in the open area of the module, and detectors in racks that have cooling air-flow (McKinnie, 1997).

The design developed for the ISS by Allied Signal™ (figure 2) consists of a 2-pass laser diode to sense forward scattered light (30 degrees). There is also a zero degree obscuration system that is used as a measure of the beam strength. The system is designed to alarm based on the magnitude of the scattered light signal referenced to the beam intensity. Some level of dust discrimination is provided based on frequency analysis of the scattered light signal. The system is less sensitive to particles smaller than the wavelength of the laser (near IR) than it is to larger particles. The minimum reported sensitivity is 0.3 μm (Steisslinger et al 1993). It draws relatively little power (1.5 W) and it has a long operational life. The current alarm value of 2 volts is calibrated to 3.3% obscuration / meter (1% obscuration / foot) of visible light for punk type smoke in a UL smoke box. In this standard smoke detector qualification method, the detector is placed in a chamber filled with smoke which is adjusted to achieve a target level of attenuation of visible light passing between a lamp and a photocell in the box (Underwriters Laboratory, UL-268, 2003).

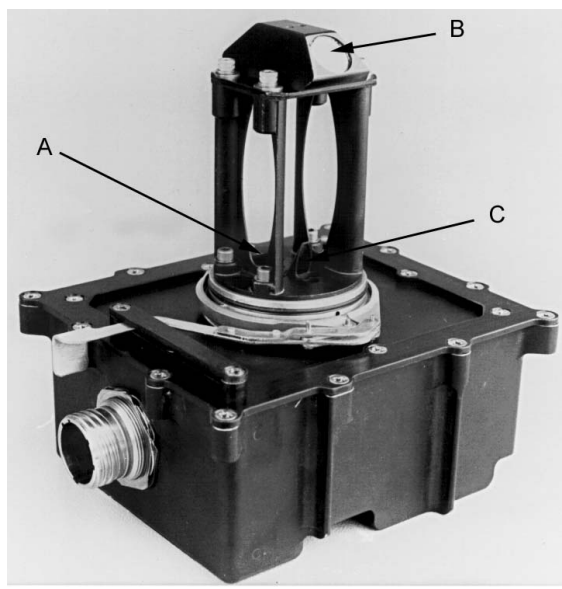

Figure 2: Allied Signal/Honeywell light-scattering smoke detector used in the ISS. The near IR laser beam emerges from the enclosure into the top assembly (A) and is reflected by two mirrors (one visible at top right (B)) and is then reflected back to the sensors in the enclosure (C). One sensor detects the forward scattered light and is referenced by another sensor that looks directly at the incident beam.

It is interesting to note that the ISS and the Orbiter detectors have particle sensitivities that are nearly

mutually exclusive. In both cases the designs were based upon the best available data however, due to the complete absence of low-g data concerning the nature of particulate and radiant emission from incipient and fully developed low-g fires, different conclusions were drawn concerning the optimal design for spacecraft fire detection.

As described by Friedman (1994) there have been six overheat and failed component failures in the NASA Orbiter fleet (Space Transportation System or STS). None of these events spread into a real fire but as mission durations increase, the likelihood of failures increases. The experience on Mir in 1997 has shown that failure of oxygen generation systems can have significant consequences. As a result, improved understanding of spacecraft fire detection is critically needed (Ruff et al., 2005).

BACKGROUND IN LOW GRAVITY SMOKE – Other than the results reported here, the only combustion-generated particulate samples that have collected near the flame zone for well-developed microgravity flames have been soot sampled from the Laminar Soot Processes (LSP) experiment (Urban et al. 1998). All of the other data either came from drop tower tests and therefore only corresponded to the early stages of a fire or were collected far from the flame zone. The fuel sources in the drop tower tests were restricted to laminar gas-jet diffusion flames (Ku et al. 1995) and very rapidly overheated wire insulation (Paul et al. 1993) and Srivastava, McKinnon and Todd (1998). The gas-jet tests indicated, through thermophoretic sampling, that soot primaries and aggregates (groups of primary particles) in low-gravity may be significantly larger than those in normal gravity (1-g). This raises new scientific questions about soot processes as well as practical issues for particulate size sensitivity and detection/alarm threshold levels used in on-orbit smoke detectors. The overheated wire insulation tests in the 2.2 second drop tower suggest that particulate generated by overheated wire insulation may be larger in low-g than in 1-g (Paul et al. 1993). One of the most surprising results was the determination by Srivastava, McKinnon and Todd (1998) that the Teflon wire coloring agent had a very strong effect on the particle size distribution and morphology. Transmission Electron Microscope (TEM) grids downstream of the fire region in the Wire Insulation Flammability experiment (Greenberg, Sacksteder and Kashiwagi 1995) as well as visual observation of long string-like aggregates, further confirm this suggestion. Subsequently, the LSP experiment sampled soot from ethylene and propane gas jet diffusion flames in long-term low gravity (Urban et al, 1998) the soot primary particles were typically twice the size of soot from similar normal gravity flames and the aggregates were more than an order of magnitude larger. The combined impact of these limited results and theoretical predictions is that, as opposed to extrapolation from 1-g data, direct knowledge of low-g combustion particulate is needed for more confident design of smoke detectors for spacecraft.

SPACECRAFT ATMOSPHERE DUST BACKGROUND – Any effort to detect fires must be able to discriminate against the ambient background and nuisance signals. In the case of smoke detection the background dust aerosol conditions must be considered. The only spacecraft background aerosol particulate measurements to date were made on the Orbiter on STS 32 in 1990 (Liu et al. 1991). These measurements included the results from two cascade impactors and a light scattering device. The two impactors reported a bimodal particle size distribution with ~ 40% of the particles in each of the 2.5 to10 μm and >100 μm ranges. The other two ranges <2.5 μm and 10 to 100 μm were very lightly populated (Table 1). Each impactor samples approximately 15 m^3 of air over approximately 30 hours. These results showed substantially higher concentrations than typical indoor measurements. These data were supported by the light scattering instrument which made 17 measurements in 12 locations, all of these reported mass concentrations ranging from 50 to 70 $\mu g/m^3$.The low particle levels in the < 2.5 μm bin suggest a zone of opportunity for spacecraft fire detection since typical normal gravity fires produce substantial particulate in this size range (Bukowski et al. 2003, Bukowski and Mulholland 1978), and the average sizes that were recorded by CSD (below) are in this size range. However more complete particle size statistics are needed.

Sample Location	Particle Size Range				
	<2.5μm	2.5-10 μm	10-100 μm	>100 μm	Total
	Mass Concentration, $\mu g/m^3$				
Shuttle	2.3	24.1	4.8	28.1	59.3
Shuttle	2.1	13.4	6.2	31.8	53.5
Home	3.0	3.0	1.0	1.5	8.5
Office	3.4	3.2	2.7	1.9	11.2
Laboratory	2.9	4.8	2.0	2.4	12.1
	Average Mass Concentration $\mu g/m^3$				
Ave. Shuttle	2.2	18.7	5.5	30.0	56.4
Ave. Indoor Environment	3.1	3.7	1.9	1.9	10.6
	Ratio of Mass Concentrations				
Shuttle/Indoor	0.71	5.1	2.9	15.8	5.3

Table 1: Airborne Particle Mass Concentration: Comparison of STS-32 to Indoor Environments (from Liu et al., 1991)

CSD EXPERIMENT

The Comparative Soot Diagnostics (CSD) experiment was conceived as an opportunity to examine smoke detection from conditions resembling incipient fires in low-gravity. Materials representative of those used in spacecraft (paper, Teflon™, Kapton™ and silicone rubber, and candle wax (representative hydrocarbon)) were heated or ignited in a few cases to produce three types of smoke (soot, recondensed liquid pyrolysis products and recondensed solid pyrolysis products). The smoke from these sources was exposed to spacecraft

smoke detectors and physically sampled for Transmission Electron Microscope (TEM) analysis. As will be described below the tests were generally successful and produced unique results. The CSD experiment flew in the Orbiter mid-deck on the US Microgravity Laboratory-3 (USML-3) mission (STS-75).

CSD EXPERIMENTAL CONCEPT - The CSD experimental hardware consisted of two modules named the Near-Field Module and Far-Field Box as shown in figure 3. The Near-Field Module (figure 4) was installed inside the Glovebox and contained the sample and the near field diagnostics. The Far-Field Box (figure 5) was external to the Glovebox and contained two spacecraft smoke detectors. Products from the near field tests were transported to the Far-Field Box and subsequently back into the Glovebox via Teflon hoses which entered the Glovebox through ports in the airlock door. All of the combustion products were contained in either the Glovebox or the Far Field Box; by the time the experiment was completed, all of the products were returned to the Glovebox.

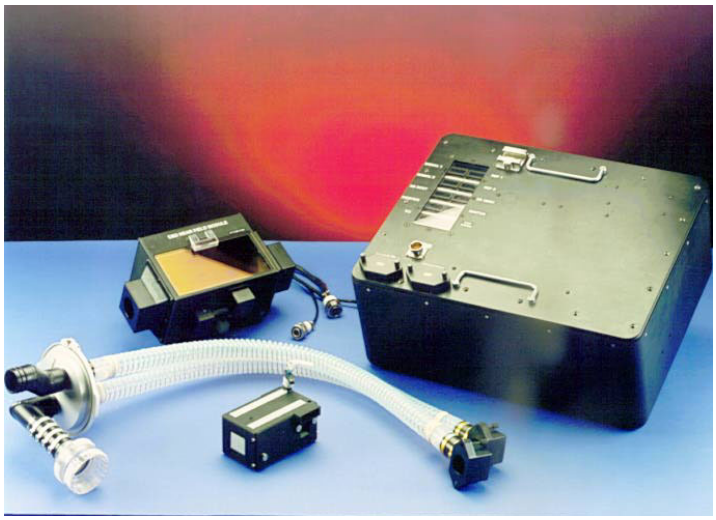

Figure 3: CSD Hardware: The Near Field Module is to the back left and the Far Field Box is to the right. Connecting hoses and thermophoretic sampler are in the front.

The Near-Field Module (figure 4) consisted of a small test chamber fitted with a sample carrier that held the sample being tested. A small fan blew air from the Glovebox into the right side of the chamber past the sample and out the left side where it entered the hose to the Far-Field Module. The sample was ignited or overheated by a resistively heated Kanthal™ wire. The smoke particulate was sampled by a rake of thermophoretic probes and smoke production was detected by a laser light extinction system.

The Far Field Box (figure 5) contained a duct and a fan to transport the smoke from the Near Field Module to two spacecraft smoke detectors, one matching the STS detector and the other identical to the ISS detector except that its signal was amplified by a factor of 6.6 over the ISS standard (due to misdiagnosed low-signal from a prior engineering model). The analog signals from the various instruments were displayed by digital readouts on the Far Field Box where they were recorded by a video camera for later transcription.

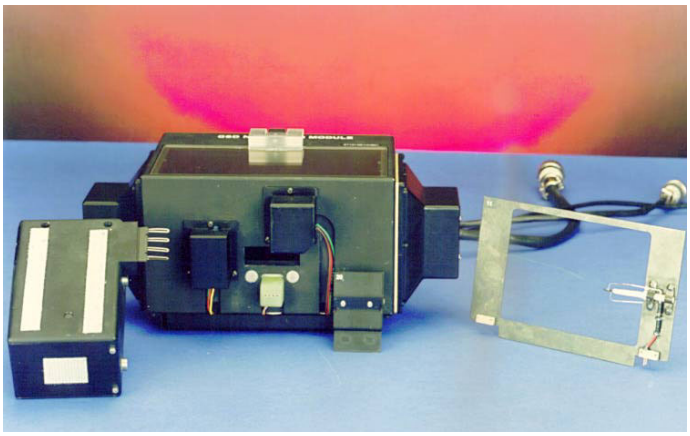

Figure 4: Near Field Module: Deployed thermophoretic probe on left and a sample card holding a candle to the right.

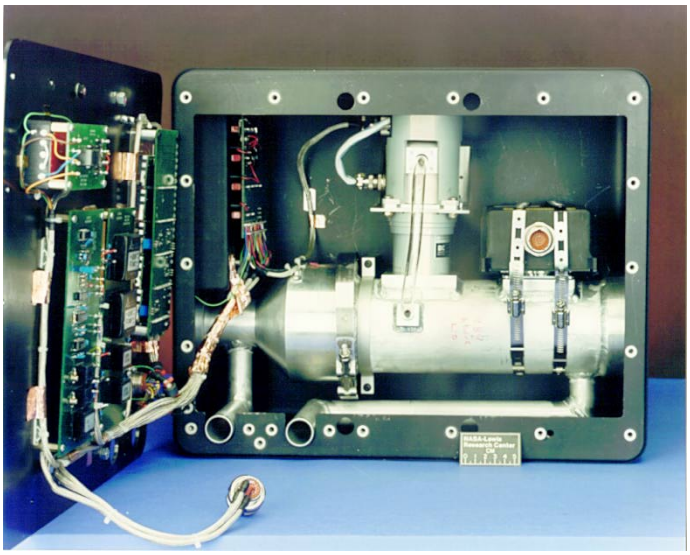

Figure 5: Interior of Far Field Box: Visible is the interior duct with the ISS detector on the right and the STS detector in the center.

CSD EXPERIMENTAL PROCEDURE - The crew installed the near field hardware in the Glovebox, attached the Far Field Box to the Glovebox, and positioned the video cameras. The operator then ran the self diagnostic procedures on the two smoke detectors and activated the video cameras, turned on the igniter for a predefined period of time (15 to 60 seconds), and initiated the thermophoretic soot samplers to sample the smoke. The actual duration of each combustion event was typically 2 minutes. After flight, the particulate collected on the thermophoretic probes were analyzed using a Transmission Electron microscope (TEM) to determine primary and aggregate particle dimensions.

The remains of the samples were weighed to determine their mass loss. The digital data was transcribed from the video record and analyzed to determine the response of the detectors. Once the flight mass loss rates were determined, 1-g operation conditions to produce the same loss were determined.

CSD EXPERIMENTAL RESULTS - In all, 25 tests were performed, the bulk of which were overheated material tests in which the heating level was established to produce a target weight loss rate without causing the sample to develop a sustaining combustion reaction. The intent of these tests was to produce smoke typical of an incipient fire where much of the material is being heated but has not yet ignited. The candle tests and one of the paper tests were combustion tests where the samples were ignited so the combustion products could be observed.

As discussed in the introduction, smoke encompasses various types of aerosol materials. In this experiment, the smoke sources can be divided into three types based upon the type of smoke that they emitted: the candle and burning paper produced soot, the Teflon™ and Kapton™ produced particles composed of solid, recondensed, pyrolysis products and the silicone rubber and pyrolyzing paper produced liquid droplets of pyrolysis products. TEM images of the solid particulate are presented below and will be discussed later. For the candle tests, the duct air flow was used to drive the candle flame past the smoke point, causing it to emit soot. These soot tests produced varied results between the two detectors as shown below (figures 6 and 7). In figure 6, both detectors showed rapid detection of the soot. In the case of figure 7, the STS detector shows a strong signal while the ISS detector signal is quite weak considering this signal has a higher amplification level than the standard detector.

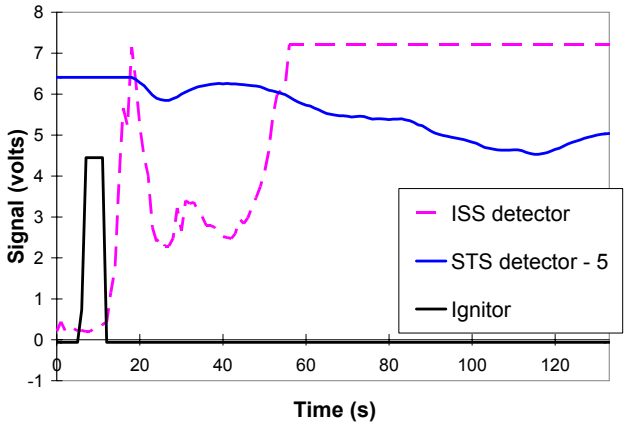

Figure 6. CSD results from candle test 16: Traces of smoke detector signals as a function of time for a candle test 16. The initial peak on both detectors is wax vapor released by the ignition process. The STS detector (solid line) shows downward deflection with increased smoke level, the ISS detector (dashed line) deflects upward.

Testing with the Teflon™ and Kapton™ produced lower overall smoke concentrations. In the case of the Kapton tests, the STS detector showed an early peak followed by a rapid return to baseline while the ISS detector reported signal for another minute (figure 8). This result may be an artifact of the flow environment or a result of the fact that the Kapton wire used on the Orbiter uses a combination of Kapton™ and Teflon™ layers and so the STS detector may be responding to only one of these materials. Similar results were seen with the Teflon™ testing (figure 9).

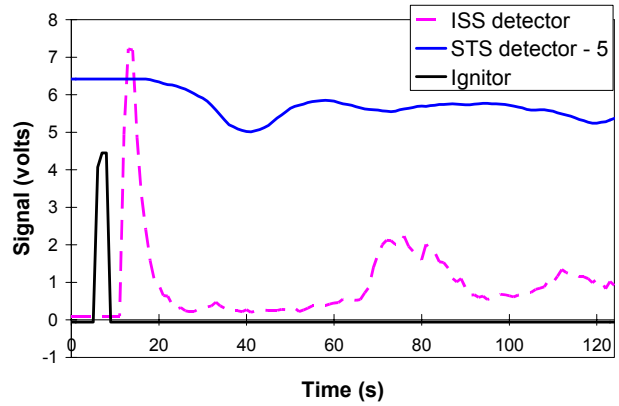

Figure 7. CSD results from candle test 6: Traces of smoke detector signals as a function of time for a candle test 6. The initial peak on both detectors is wax vapor released by the ignition process. The STS detector (solid line) shows downward deflection with increased smoke level, the ISS detector (dashed line) deflects upward.

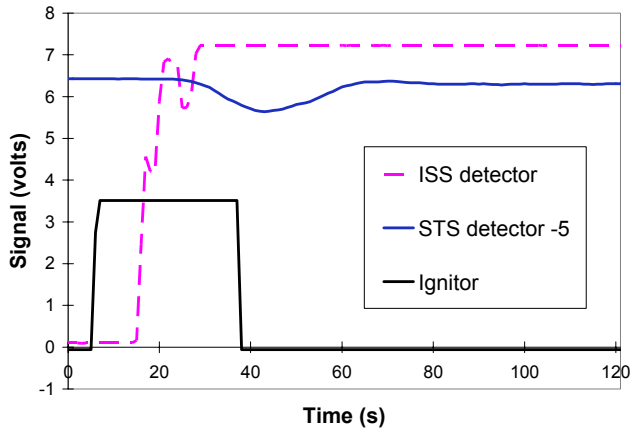

Figure 8. CSD results from Kapton™ test 9: Traces of smoke detector signals as a function of time for a Kapton™ test 9. The STS detector (solid line) shows downward deflection with increased smoke level, the ISS detector (dashed line) deflects upward.

The liquid smoke producing samples produced very different results as seen in figure 10 for the silicone

rubber. Despite producing dense smoke that was clearly visible, the STS detector showed virtually no signal while the ISS detector saturated.

The approach for the pyrolyzing paper samples was to heat them below the ignition temperature so they produced smoke without ignition. This produced similar results to the silicone rubber with virtually no signal on the STS detector and a strong signal on the ISS detector. Notably in one test the sample ignited and the STS detector signal changed from the baseline to a substantial peak (figure 11) presumably because the smoke now contained soot in addition to the condensed pyrolysis products.

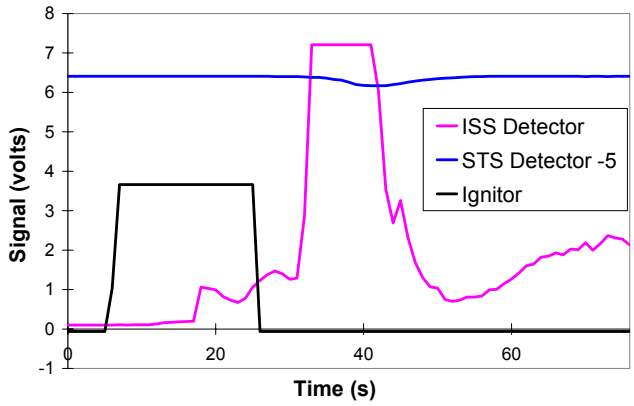

Figure 9. CSD results from Teflon™ test 13: Traces of smoke detector signals as a function of time for a Teflon™ test 3. The STS detector (solid line) shows downward deflection with increased smoke level, the ISS detector (dashed line) deflects upward.

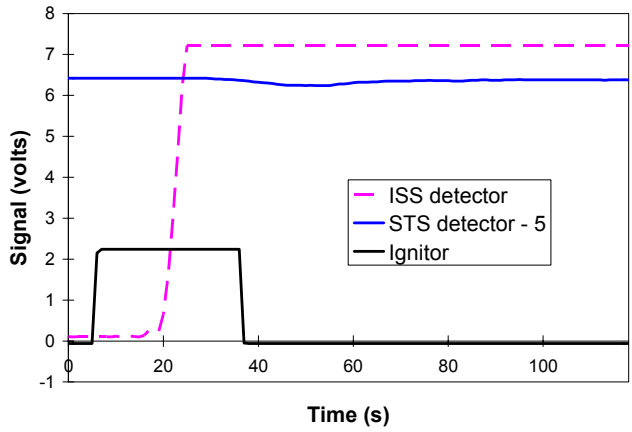

Figure 10. CSD results from silicone rubber test 7: Traces of smoke detector signals as a function of time for a silicone rubber test 7. The STS detector (solid line) shows downward deflection with increased smoke level, the ISS detector (dashed line) deflects upward.

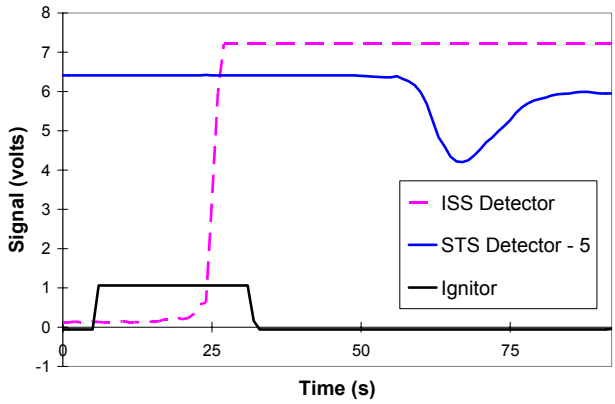

Figure 11. CSD results from paper test 15: Traces of smoke detector signals as a function of time for a paper test 15. The STS detector (solid line) shows downward deflection with increased smoke level, the ISS detector (dashed line) deflects upward. The onset of signal for the STS detector correlated with ignition of the paper.

Figure 12 contains TEM images of typical particulate from Teflon, Kapton and Candle tests. The three images are at the same magnification and show the significant variation in the particulate morphology for the three materials. The Teflon and Kapton particulate are recondensed polymer material while the candle particulate is typical of hydrocarbon soot. Table 2 summarizes the results for the tests for which comparable particulate samples were collected for 1-g and low-g. Significantly, despite strong smoke levels visible in the video record, no particulate material was found on the TEM grids for overheated paper and silicone rubber tests. The suspected cause of this is that the particulate for these materials is actually liquid droplets which later evaporated or spread out on the grids' surface, rendering them undetectable by the TEM

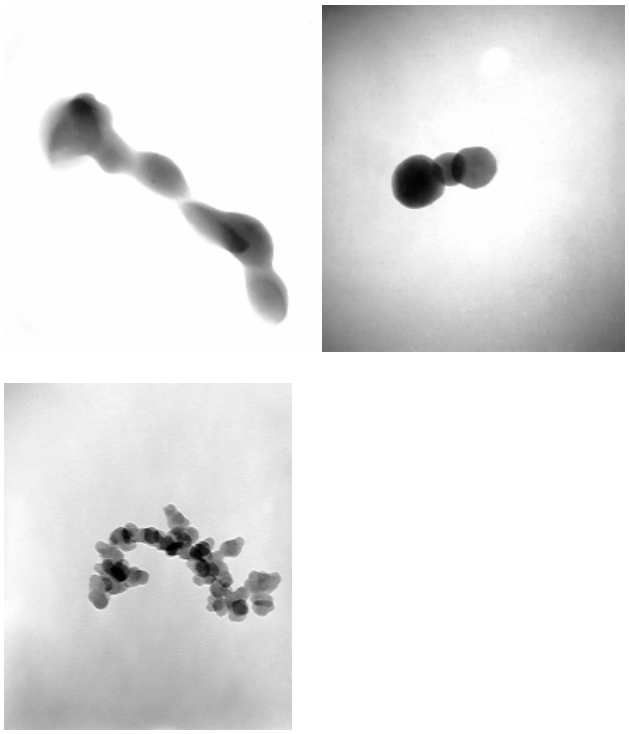

Figure 12. Transmission Electron Microscope Images of smoke particles from Teflon, Kapton (left to right, top row) and Candle tests (bottom). Images are at the same magnification, for scale reference: candle soot primary particles are approximately 20 nm.

Table 2: Geometric mean diameters for smoke particulate generated in reduced gravity and in normal gravity.

	Primary Particles (nm)		Aggregate Length (nm)	
Material	Low-g	1-g	Low-g	1-g
Kapton	76	35	223	35
Candle	34	17	976	265
Teflon	136	75	662	277

The experiment was not configured to reproduce fire scenario particulate levels, and the ISS detector was more sensitive than the ISS standard, consequently tabulation of successful alarms is not straight forward. Since the experiment was developed as a test of light scattering versus ionization technology rather than a test of the detectors themselves, the standard that was selected to indicate successful detection of the smoke from the background was a signal that was 20% of the device operating range. Using these criteria, the results are reported in table 3.

Table 3: Summary of runs where the smoke was detected by the ISS and STS detectors.

	Test Runs		
Material	Total	Detected by ISS detector	Detected by STS detector
Paper	5	2	1
Candle	4	3	2
Silicone Rubber	5	5	0
Teflon	6	3	2
Kapton	5	4	4

In general the light scattering detector was more successful at detecting the smoke particulate, particularly for the cases where the smoke was a liquid aerosol (paper and silicone rubber). The results were more mixed for the cases where the particulate was solid particles. The improved performance by the ISS detector for the solid particulate is readily explained by the large particle sizes reported in table 2. Unfortunately for the liquid particulate, no particle sizes were obtained because the liquid droplets on the TEM grids evaporated before the grids could be evaluated in the TEM. Based upon these results, the need for an experiment that could measure properties of the smoke particulate size distribution on-orbit was established and a new experimental concept was developed as described below.

SAME EXPERIMENT

Although the CSD experiment produced useful information concerning the likely size of spacecraft smoke particulate, the data set was not particularly large as the size statistics were obtained from TEM data and critical details were not obtained for the liquid droplet aerosols. To rectify this concern, another experiment (Smoke Aerosol Measurement Experiment: SAME) is under development. The SAME experiment seeks to avoid the problems seen by the CSD experiment by obtaining the particulate size statistics on-orbit without as much dependence upon sample return to Earth. This is a challenging endeavor because most existing aerosol instrumentation is typically large, requires large sample sizes and would require substantial sample return to Earth. As will be described below, an alternate approach using three discrete instruments that will measure separate moments of the size distribution will be used. When combined, these moments will provide useful aggregate statistics of the size distribution.

The measurements will be made using smoke generated by overheated spacecraft materials in much the same manner as the CSD experiment however the sample temperature, flow field, and particle aging time will be more rigorously controlled.

MOMENT METHOD – The approach used by the SAME experiment is termed the 'moment method' for convenience. As will be described below, the approach consists of measuring three moments of the size distribution (zeroth, first and third) and using the properties of the log-normal distribution to estimate the geometric mean diameter and the standard deviation.

The average particle size and an estimate of the width of the size distribution will be estimated from various moments of the size distribution. The number distribution, $f_N(D)$, is defined as

$$f_N(D) = \frac{dN}{dD} \qquad (1)$$

where dN is the number of particles per cm^3 with diameter between D and D + dD. The moments of interest consist of the number concentration, M_0, the first moment M_1, and the volume or mass concentration moment, M_3.

$$M_i = \int D^i f_N(D) dD \quad i = 0,1,3 \qquad (2)$$

The first moment which can also be thought of as the "diameter concentration" or integrated diameter per unit volume is largely proportional to the ionization detector moment (signal). For particles in the Mie scattering regime, particles sizes from 0.3λ to about 3λ the light scattering signal is proportional to the third moment. From these moments, two mean diameters can be computed: the arithmetic mean diameter ($D_{0.5}$) or $(\overline{d})$, which is equal to M_1/M_0 and the diameter of average mass ($D_{1.5}$) or $(d_{\overline{m}})$, which is equal to $(M_3/M_0)^{1/3}$. The log-normal size distribution is widely used for describing the size distribution of aerosols including both flaming and non-flaming smoke as in most aerosols; the bulk of the number concentration is associated with smaller particles (Raabe, 1971 and Reist, 1984). In the case of bimodal distributions, the log-normal distribution still captures the overall distribution with a larger standard deviation. The form of the distribution is the same as the normal distribution except that the diameter is replaced with the ln D so that one has

$$f_N(D) = \frac{N_t}{(2\pi)^{1/2} D \ln \sigma_g} \exp\left(-\frac{\ln D - \ln D_g}{2 \ln^2 \sigma_g} \right) \qquad (3)$$

where N_t is the total number concentration of the aerosol (=M_0), and D_g and σ_g are the geometric mean number diameter and geometric standard deviation defined by

$$\ln D_g = \int_0^\infty \ln D f_N(D) dD \Big/ \int_0^\infty f_N dD \qquad (4)$$

$$\ln \sigma_g = \left[\int_0^\infty (\ln D - \ln D_g)^2 f_N(D) dD \Big/ \int_0^\infty f_N(D) dD \right]^{1/2} \qquad (5)$$

For the log-normal distribution, one finds that the various diameter definitions are related to the geometric mean number diameter, Dg, via the equation [Raabe, 1971, Reist, 1984]:

$$D_p = D_g \exp(p \ln^2 \sigma_g) \qquad (6)$$

For the arithmetic mean diameter, $D_{0.5}$, and the diameter of average mass, $D_{1.5}$, the corresponding values of p are 0.5 and 1.5. As an example, for a log-normal distribution with D_g=1.0 μm and σ_g=2.0, the corresponding values of $D_{0.5}$ and $D_{1.5}$ are1.27μm and 2.06 μm. Using equation (4), one can relate σ_g to the ratio of $D_{1.5}$ and $D_{0.5}$ via the equation:

$$\sigma_g = \exp\left(\ln(D_{1.5} / D_{0.5})\right)^{1/2} \qquad (7)$$

By combining these three moments it is possible to compute three mean diameters of the size distribution and the geometric standard deviation. Validation of this approach is discussed in Cleary, Weinert and Mulholland (2003). These statistics provide a strong basis for design of spacecraft smoke detectors.

INSTRUMENTS – These measurements will be made using an assembly of three separate instruments. Two are industrial hygiene instruments manufactured by TSI™ and one is a modified residential smoke detector.

The zeroth-moment instrument is a condensation nuclei counter "P-Trak™" manufactured by TSI™. This device operates by passing the aerosol laden particle stream through a region where it is saturated with isopropanol vapor and then into a cooler region where the vapor condenses onto the particles raising them all to a size where they are readily counted by a light scattering device. This instrument is very robust and operates over a range of 0 to 10^5 particles/cm^3 and 20 nm to 1 μm diameter. However, as will be described below, there is a concern that the isopropanol condensate will not return to the wick in low-gravity.

The first-moment instrument is the ionization chamber from a residential smoke detector. The devices use an alpha-particle emitter to generate ions in a region inside a DC electric field which causes the ions to drift producing current. Aerosol particulate that enters the chamber attaches to some of the ions, increasing their mass and thereby reducing their mobility and the current. The required particle concentrations are on the order of 10^5 particles / cm^3 so the other moment instruments will need to sample a diluted smoke stream compared to the ionization chamber.

The third-moment instrument is a light scattering device "DustTrak™" manufactured by TSI™. The device uses a 90 degree light scattering signal to quantify the aerosol mass density. For terrestrial dust particulate this signal correlates well with the mass concentration, however additional compensation will be needed to account for the range of particle sizes that will be seen in the SAME experiment. The device operating range is from 0.001 to 100 mg /m^3

DAFT EXPERIMENT

To reduce the risk of the SAME experiment, it was determined that an early test of the operation of a P-Trak™ in low-gravity was desirable. To accomplish this, an experiment was developed that would use a P-Trak™ and DustTrak™ on the ISS to test the ambient air and an aerosol calibration source. At this point, the entire experiment has not been conducted but initial results from tests with the DustTrak™ and P-Trak™ for the ISS cabin during Expedition 10 are available. This is a notable result since these are the first measurements of the particulate aerosol concentration on the ISS.

INSTRUMENTS - The instruments were a Dust Trak™ (figure 13) and a P-Trak™ (figure 14). The P-Trak™ a type of Condensation Nuclei Counter (CNC) was modified with microgrooves in the condenser to increase the alcohol transport back to the wick. The Dust Trak™ was unmodified other than typical flight hardening.

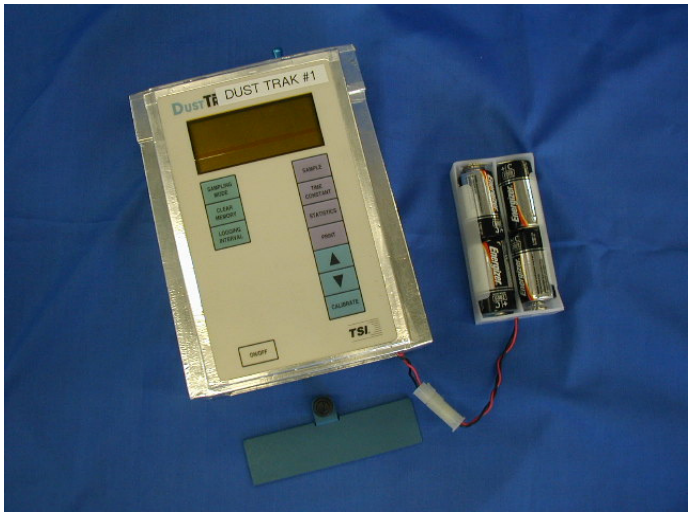

Figure 13: TSI™ Dust Trak™ prepared for flight. Battery compartment is open showing the battery pack.

Figure 14: TSI™ P-Trak™ prepared for flight. Clockwise from left: alcohol wick, wick container, wick container lid, P-Trak™, battery pack.

RESULTS – Only four tests have been run to date. Further tests will be conducted when other components are launched on future flights. The procedure for each test was to activate both instruments, attach a HEPA (High Efficiency Particulate Air) filter to the inlet to produce a zero baseline, connect the instruments to a common sampling hose, record the environment for several minutes and then reconnect the HEPA filters for another baseline and then shutdown the instruments. Total run time was limited due to the alcohol release from the CNC device. Tests were conducted on February 22, 2005 in the US Lab in front of Express Rack 4 and on March 4, 2005, in the US Lab, aft end, port side and in the node. Three tests sampled undisturbed cabin air and one test was used to validate the instruments at high particulate levels by deliberately separating Velcro™ at the device inlets.

Contrary to the high particulate levels seen in the space Orbiter, all three tests that sampled the undisturbed environment showed very low levels, (average less that 0.005 mg / m^3 from the DustTrak™ and less than 15 particles /cm^3 from the P-Trak™ with typical readings at the zero baseline for both instruments. This is dramatically lower than the values recorded on the Orbiter (~ .050 mg / m^3) (Table 1) by Liu et al. (1991). These lower levels are to be expected because the ISS US lab has HEPA filtration for the cabin air compared to a fine screen on the Orbiter air handler. Furthermore, the typical Orbiter crew of 7 can be expected to generate much more particulate than the current ISS crew of 2. Further measurements are needed at more locations in the ISS as these limited observations cannot represent the entire vehicle air volume. In fact as the test was being initiated on March 4, 2005 a smoke detector in the Russian segment (ionization device) triggered its alarm indicating high particulate levels in its location. Nevertheless, these low levels on the ISS suggest that the particulate baseline level should be expected to

reach low levels in sparsely crewed vehicles with extensive air filtration.

CONCLUSION

Reliable detection of microgravity fires will require use of systems whose design is based upon thorough understanding of microgravity fire phenomena and the ambient environment on the spacecraft. The ISS and the Orbiter have dramatically different air filtration systems with the result that the ambient air varies from substantially more particulate than typical on earth (Orbiter) to substantially cleaner than a terrestrial office building (ISS). Limited testing to date has shown that low-gravity conditions favor substantial smoke particle growth and the particulate size distribution for smoke from low-gravity fires can be 2 to 8 times larger than in normal gravity. Variations of this magnitude must be considered in future detector design which must also be coupled with an understanding of the performance of the air filtration systems.

ACKNOWLEDGMENTS

The authors acknowledge the contributions of the crews of STS-75, ISS Increment 10 and the CSD and DAFT teams.

Certain commercial entities, equipment, or materials may be identified in this document in order to describe an experimental procedure or concept adequately. Such identification is not intended to imply recommendation or endorsement by the National Aeronautics and Space Administration or the National Institute of Standards and Technology, nor is it intended to imply that the entities, materials, or equipment are necessarily the best available for the purpose.

REFERENCES

Bukowski, R.W. and G.W. Mulholland., 1978. Smoke Detector Design and Smoke Properties. NBS Technical Note 973.

Bukowski, R. W, R. D. Peacock, J. D. Averill, T. G. Cleary, N. P. Bryner, W. D. Walton, P. A. Reneke, and E. D. Kuligowski, 2003. Performance of Home Smoke Alarms, Analysis of the Response of Several Available Technologies in Residential Fire Settings NIST Technical Note 1455, December.

Cleary, T.G., D W. Weinert, and G.W. Mulholland, 2003."Moment Method for Obtaining Particle Size Measures of Test Smokes", Natl. Inst. Stand. Technol., NISTIR 7050.

Friedman, R., 1992. Fire Safety Practices and Needs in Human-Crew Spacecraft, Journal of Applied Fire Science, 2:243-259.

Friedman, R., 1994. Risks and Issues in Fire Safety on the Space Station, NASA TM 106430.

Ku, J.C., D.W. Griffin, P. S. Greenberg, , and J. Roma, 1995: Combustion and Flame, 102:216-218.

Greenberg, P. S., K. R. Sacksteder and T. Kashiwagi. 1995. Wire Insulation Flammability Experiment, NASA CP 3272 V II.

Liu, B. Y. H., K. L. Rubow, P. H. McMurry, T. J. Kotz and D. Russo. 1991. Airborne Particulate Matter and Spacecraft Internal Environments, SAE Technical Paper 911476, 21st International Conference on Environmental Systems, San Francisco, CA , July 15-18.

McMurry, T., J. Kotz and D. Russo. 1991. Airborne Particulate Matter and Spacecraft Internal Environments, SAE Technical Paper 911476, 21st International Conference on Environmental Systems, San Francisco, CA , July 15-18.

Martin, C.E. and R.C. DaLee, 1993. Spacecraft Fire Detection and Suppression (FDS) Systems: An Overview and Recommendations for Future Flights, SAE Technical Paper 932166, 23rd International Conference on Environmental Systems, Colorado Springs, CO, July 12-15.

McKinnie, J., 1997. Fire Response Aboard the International Space Station, SAE Technical Paper 972334, 27th International Conference on Environmental Systems, Lake Tahoe, NV, July 14-17.

National Research Council, 1975. Fire Detection for Life Safety, National Academy of Sciences, Washington D.C.

Paul, M., F. Issacci, G. E. Apostalakis and I. Catton. 1993. ASME-HTD Vol. 235:59-66.

Raabe, O.G., J. Aerosol Sci., 1971. 2: 289.

Reist, P.C. 1984, Introduction to Aerosol Science. Macmillan Pub. Co., NY, NY.

Ruff, G.A., D.L. Urban, and M.K. King, "A Research Plan for Fire Prevention Detection and Suppression," AIAA-2005-0341, 43rd Aerospace Sciences Meeting and Exhibit, Reno, NV, January 9-12, 2005.

Srivastava. R., J.T. McKinnon and P. Todd, 1998. Effect of Pigmentation in Particulate Formation from Fluoropolymer Thermodegradation in Microgravity, AIAA 98-0814, Aerospace Sciences Meeting, Reno NV, Jan 12-15.

Steisslinger, H. R., D. M. Hoy, J. A. McLin and E. C. Thomas., 1993. SAE Paper 932291.

Underwriters Laboratory, 2003. Smoke Detectors of Fire Alarm Signaling Systems, UL Standard 268.

Urban, D.L., Z.-G. Yuan, P.B. Sunderland, G.T. Linteris, J.E. Voss, K.-C. Lin, K. Sun and G.M. Faeth, 1998. Structure and Soot Properties of Nonbuoyant Ethylene/Air Laminar Jet Diffusion Flames, AIAA Journal, V36 p1346-1360.